Korean J. Chem. Eng., 33(5), 1674-1680 (2016)
DOI: 10.1007/s11814-016-0006-9

pISSN: 0256-1115
eISSN: 1975-7220

Intelligent identification of the flow regimes of two-component particles in a fluidized bed with the optimized fuzzy c-means clustering algorithm

Heng Wang*, Zhaoping Zhong*,†, Xiaoyi Wang, and Feihong Guo***

*Key Laboratory of Energy Thermal Conversion and Control of Ministry of Education, School of Energy and Environment, Southeast University, Nanjing 210096, China
**Engineering Design & Research Institute, Southeast University, Nanjing 210096, China
(*Received 10 June 2015 • accepted 6 January 2016*)

Abstract−Flow regime identification is important in the application of fluidized beds. This paper provides a method for deciding flow regime number by objective criterion. The optimized fuzzy c-means clustering algorithm was used to cluster the flow regime classification of two-component particles in a fluidized bed. The genetic algorithm was applied to optimize the initial center clusters of fuzzy c-means clustering. Hilbert-Huang transform was applied to analyze pressure fluctuation signals and extract the characteristic parameters. Three clusters were found and respectively ascribed to three flow regimes: bubbling bed, slugging bed, and turbulent bed. A multilayer neural network was used to train and test the identification system of the flow regimes. The identification accuracies of bubbling bed, slugging bed, and turbulent bed can reach 91.67%, 92.85%, and 91.30%, respectively.

Keywords: Fluidization, Flow Regime Identification, Fuzzy C-means Clustering, Two-component Particles, Hilbert-Huang Transform

INTRODUCTION

With the development of gas-solid fluidized bed reactors, biomass energy is widely applied in combustion, pyrolysis, and gasification. In these industrial applications, biomass materials do not have an ideal fluidized performance due to the large size and low density. Fluidized medium such as quartz sand can optimize the fluidized performance of biomass when the medium is mixed with the biomass particles. The fluidization of two-component particles is more complex than that of one-component in a gas-solid fluidized bed. Duan et al. [1] identified different flow patterns of the mixture of quartz sand with Geldart group B or group D by analyzing pressure fluctuations with Shannon entropy analysis method. Choi et al. [2] investigated the type of transition in onset condition of turbulent fluidization in gas fluidized beds to obtain the relation of physical properties of gas and solid particles. Fotvat et al. [3] investigated the effect of biomass particles on the gas distribution and the fluidized characteristics of sand-biomass particles in the gas-solid fluidized bed. Llauro et al. [4] classified the flow regimes of FCC in a fluidized bed by analyzing the pressure fluctuation signals with non-linear methods. It is necessary to completely study the flow regime identification of two-component particles in a gas-solid fluidized bed. Generally, the types of flow regimes in fluidized bed are described as fixed bed, bubbling bed, turbulent bed, slug bed, fast bed (only in circulating fluidized bed) and pneumatic transport (strictly, not used in fluidized bed). However, the flow regime classification is controversial on the basis of various analyses [5-7]. Jaiboon et al. explored different flow regimes of semi-circulating fluidized beds by analyzing the pressure fluctuation signals with power spectral density [8]. Wang et al. [9] provided a method to explore the flow regimes of spouted beds based on the analysis of pressure fluctuation signals. The conclusions of previous researches depending on direct observation are different with different experimental conditions and apparatuses. To classify the flow regimes objectively, an optimal number was introduced in this paper.

Clustering methods have been applied in system design, clustering and feature analysis and other engineering fields extensively [10]. Fuzzy c-means clustering algorithm is one of the classical unsupervised classification solutions to classify the samples into different clusters [9]. However, the clustering results may converge to the local minimization because the initial clustering center is randomly selected. This problem can be solved by applying the genetic algorithm before clustering. Instead of choosing the initial clustering center randomly, the initial clustering is calculated by the genetic algorithm to avoid the local minimization converge.

In this paper, the Hilbert-Huang transform was first applied to analyze pressure fluctuation signals and extract the characteristic parameters for processing with fuzzy c-means clustering algorithm. Then the genetic algorithm was adopted to optimize the initial center cluster of fuzzy c-means clustering, which significantly affected the classification results of samples. Finally, with the classification results, the neural network was used to identify the flow regimes of two-component particles in the fluidized bed.

EXPERIMENTS

The experiment was in a lab-scaled fluidized bed system shown in Fig. 1. The experimental system is composed of a gas supply sub-

†To whom correspondence should be addressed.
E-mail: zzhong@seu.edu.cn

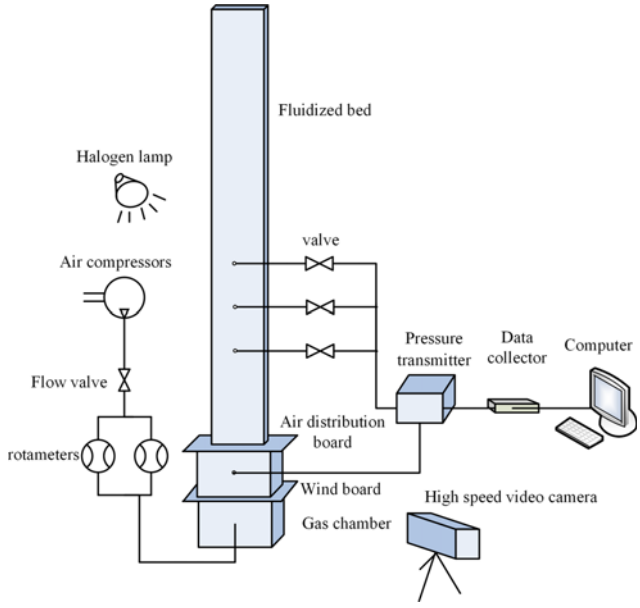

Fig. 1. Schematic drawing of fluidized bed system.

system, a data measurement and acquisition sub-system, and the main fluidized bed. The fluidized bed (120 mm×32 mm×1,000 mm) is made of 6 mm thick Plexiglas. There is a gas distributer with 126 circular holes on the bottom of the bed. The diameter of the holes is 1 mm and the total area of all holes accounts for 2.6% of the area of the gas distributer.

Several details of the gas supply sub-system are described below. An air compressor provided the fluidized gas and two rotameters were installed to control the flow velocity. The gas was delivered with braided silicone tubes (ID=30 mm) between the air compressor and rotameters. The gas passes through silicone tubes (ID= 1 mm) from the rotameters to the fluidized bed. The gas enters the fluidized bed via a gas chamber which is on the bottom of the fluidized bed and connected with the gas distributer. The gas inlet was located on the front face of the lower part of gas chamber. The gas chamber is divided into two parts by a wind board, which can reduce the perturbations of the gas injected from the air compressor and rectify the flow to make the measurement more accurate.

Table 1. Physical characteristic of particles

Particle	Bulk density	Minimum fluidized velocity	Diameter
	$kg \cdot m^{-3}$	m/s	mm
Rice husk	76	-	-
Quartz	1,350	0.56	0.5

The data measurement and acquisition sub-system is composed of a high-speed video camera for recording the images of fluidized particles at the speed of 500 pictures per second, a halogen lamp, a pressure transmitter with a data collector for obtaining pressure pulsating signals, and a computer for receiving the measured data. The pressure measurement ports on the fluidized bed are 200 mm, 300 mm, or 400 mm above the bottom of the fluidized bed. Additionally, a pressure measurement port is at the 3/4 of the gas chamber height to obtain the difference of pressure fluctuation signals. The digital camera is settled in front of the fluidized bed to catch the flow patterns during the experiments.

Rice husk, a kind of abundant biomass waste, has irregular shape and cannot be fluidized without a fluidized medium. In this experiment, the fluidized characteristic of rice husk was optimized by mixing it with quartz sand according to different mass ratios (2%, 4%, 6%, and 8%). The character parameters of particles are shown in Table 1 and the features in Fig. 2. The superficial velocity of fluidized gas gradually increased from 0.35 m/s to 1.61 m/s at the rate of 0.07 m/s and the range of superficial velocity was changed at different conditions. The minimum fluidized velocities of different mixing particles were determined by pressure drop method [11,12]. The bed height of the mixed particles was gradually changed from 100 mm to 200 mm with the interval of 20 mm. The pressure fluctuation signals were recorded with a sampling frequency of 100 Hz and at least 2^{10} data were sampled during each measurement. The samplings were gathered under the condition that the superficial velocity be above the minimum fluidized velocity. Additionally, the data of quartz sand system was sampled as comparison.

(a) (b)

Fig. 2. Particles (a) quartz sands, (b) rice husk.

THEORY

1. The Process of Empirical Mode Decomposition

The analysis methods of pressure fluctuation developed with different theories can be classified into four categories: time series analysis [13-15], frequency series analysis [16-20], time-frequency series analysis [17,21-23], and state space analysis [4,20,22,24-31]. The above-mentioned analysis methods of pressure fluctuations in fluidized beds have been reviewed [32-36]. Hilbert-Huang transform is considered as one of the applicable analysis methods for nonlinear and non-stationary process [37]. In this paper, it was adopted to transform the pressure fluctuation signals of two-component particles into characteristic parameters.

Hilbert-Huang transform (HHT) is an analysis method for a nonlinear and non-stationary time series which are chaotic and have stochastic properties [38]. HHT developed by Huang et al. [37] is based on empirical mode decomposition (EMD) and Hilbert transform. The EMD method can decompose any complicated data into several intrinsic mode function (IMF) components. Then instantaneous frequency and energy are obtained with the decomposition of IMFs by Hilbert transform.

IMFs indicate the oscillation of original data and each IMF has its own amplitude and frequency in every cycle. The time series X(t) obtained from the experiments can be decomposed first with the EMD method.

$$X(t)=\Sigma_{i=1}^{n}c_i+r_n \tag{1}$$

where $\Sigma_{i=1}^{n}c_i$ is the component of IMF_i; n means the times of decomposition; r_n is the residue of decomposition.

Fig. 3 shows the first seven IMFs of one time series obtained in the experiment. Then we can get the Hilbert transform of each IMF:

$$Y(t)=\frac{1}{n}P\int_{-\infty}^{\infty}(X(t')\ (t-t'))dt'. \tag{2}$$

With X(t) and Y(t), an analytic signal Z(t) can be described as

$$Z(t)=X(t)+iY(t)=a(t)e^{i\theta(t)} \tag{3}$$

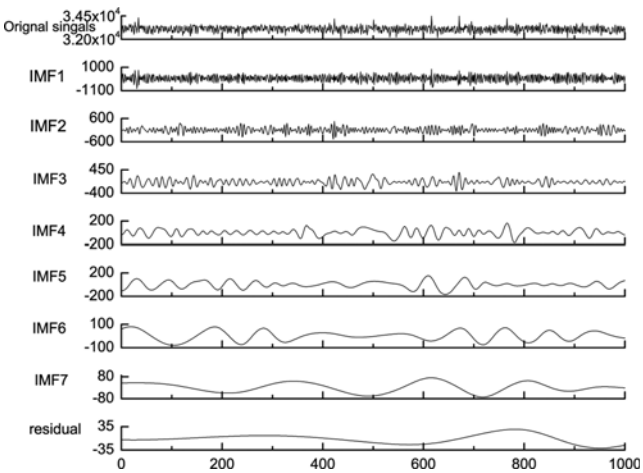

Fig. 3. IMFs of pressure signal. The result of a group of pressure signal decomposed by EMD.

where

$$a(t)=\sqrt{X^2(t)+Y^2(t)} \tag{4}$$

$$\theta(t)=\arctan(Y(t)/X(t)) \tag{5}$$

The energy of the IMF is defined as:

$$E=\Sigma_{i=1}^{n}\left|a_i^2(t)\right| \tag{6}$$

According to previous results [36,39,40], the bubble movements may be reflected by the pressure fluctuation signals. The pressure fluctuation frequency between 1 Hz and 5 Hz is defined as the medium frequency which is decomposed as $IMF_{4\text{-}6}$. The frequency below 1 Hz is the low frequency decomposed as $IMF_{7\text{-}8}$ and the frequency above 5 Hz is the high frequency decomposed as $IMF_{1\text{-}3}$. The percentages of $IMF_{1\text{-}3}$ and $IMF_{4\text{-}6}$ are used as the characteristic parameters in the next section of this paper. Additionally, $IMF_{7\text{-}8}$ represented the sum of 7th IMF and 8th IMF. The value of $IMF_{7\text{-}8}$ is so small that the cluster result would not be affected.

2. Fuzzy C-means (FCM) Clustering Algorithm

$X=\{x_1, x_2 \ldots x_N\}$ is given as a data set and each $x_i=[x_{i1}, x_{i2} \ldots x_{in}]$ consists of n measured characters. Unlike hard cluster, each x_i may be partitioned to one or more fuzzy clusters. The total number of the clusters is c.

The classical objective function of fuzzy c-means clustering algorithm was defined by Dunn [41] in 1975 and improved by Bezdek [42] in 1981 as:

$$J(X;\ U,\ V)=\Sigma_{k=1}^{c}\Sigma_{i=1}^{N}(\mu_{ki})^m\left\|x_i-v_k\right\|^2 \tag{7}$$

where U is an N×c matrix consisting of N rows: $\{\mu_{i1}, \mu_{i2}, \ldots \mu_{ic}\}$, which are the membership functions of each cluster; $V=[v_1, v_2, \ldots,$

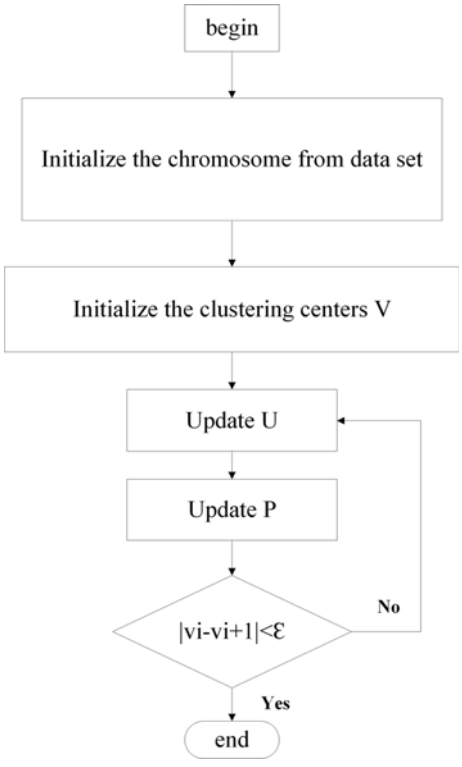

Fig. 4. The crucial steps of fuzzy c-mean clustering algorithm.

v_c] is a vector of cluster centers; $\Sigma_{k=1}^{c}\mu_{ki}=1$, i=1, 2, …, n, $\mu_{ki}\in(0, 1)$; m is the weighting exponent; μ_{ki} and v_k are given as follows, based on Lagrange multiplier:

$$\mu_{ki}=1/\Sigma_{j}^{c}(d_{ki}/d_{ji})^{2/(m-1)},\ 1\le k\le c,\ 1\le i\le N \quad (8)$$

$$v_i=\Sigma_{i=1}^{n}[(\mu_{ki})^m x_i]/\Sigma_{i=1}^{n}(\mu_{ki})^m,\ 1\le i\le c \quad (9)$$

The minimization of J is the foundation of fuzzy c-means clustering algorithm, which is a common method to solve nonlinear optimization problems. The weighting exponent m and the number of clusters c are crucial to the clustering validity.

The crucial steps of fuzzy c-means clustering algorithm involve the iteration process shown in Fig. 4.

Although FCM is applied widely, it is not applicable in some complicated cases. The limitation of FCM is that the cluster number c and the weighting exponent m should be determined before clustering, but the value of c and m is not definite in some circumstances. A validity index is referred to obtain the appropriate c and m [9]:

$$I(c, m)=\frac{1}{N}\Sigma_{k=1}^{c}\Sigma_{i=1}^{c}\mu_{ki}^{2}-\frac{1}{c}\Sigma_{k=1}^{c}(\Sigma_{i=1}^{N}\mu_{ki}^{2}/\Sigma_{i=1}^{N}\mu_{ki}) \quad (10)$$

The smaller value of I indicates the better values of c and m.

3. Genetic Algorithm

Another drawback of FCM is that the iterative algorithm always converges to the local minimization point, which is probably not the global minimization point. The result of FCM is highly sensitive to the initial clustering center. However, it is difficult to determine the center of each clustering according to experiences. In this paper, the adopted genetic algorithm is based on global optimization algorithm to find the appropriate cluster number c and the initial cluster center V. The objective function of FCM will be considered in the fitness function F of GA as:

$$F=1/[1+\Sigma_{k=1}^{c}\Sigma_{i=1}^{N}(\mu_{ki})^m\|x_i-v_k\|^2] \quad (11)$$

The larger F means the better optimized center clustering. The basic steps of the genetic algorithm are provided as follows:

Step 1. Coding: to initialize the population by random selecting each gene p_j (j=1, 2, …, c) from original data set $X=\{x_1, x_2, \ldots, x_N\}$ and then coding each chromosome $P_r=\{p_1, p_2, \ldots, p_j, p_c\}$. Additionally, r=1, 2… s and s is assigned as the size of population $P=\{P_1, P_2, \ldots, P_s\}$. G is the total number of generation. t is initialized to be 0 and regularly increased by 1 with the increase of the generation until t=G.

Step 2. Selecting the operator: the measures of replication, crossing, and mutation are applied to select the chromosome and get the new generation.

Step 3. Evaluating the new generation: the fitness function is adopted to examine the new generation. The better one will replace one of the original chromosomes to allow the minimum value of the fitness function.

Step 4. Let t=t+1 and circling Step 2 and 3 till t=G.

Step 5. Exporting the best chromosome of the last generation as the initial center clustering and running FCM.

4. Analysis of Pressure Fluctuation Signals with GA-FCM

The data set of pressure fluctuation signals was obtained from the experiment in Section 2. Three controlled variables (the percentages of biomass and quartz, the bed height, and the velocity) were considered and 200 group pressure fluctuation signals were sampled under different conditions for clustering. With the aforementioned theories, the data set was clustered according to the following steps.

Table 2. The value of I with different c and m

m	C=2	C=3	C=4	C=5	C=6	C=7	C=8
2.5	0.909	0.900	0.910	0.921	0.946	0.959	0.952
2.25	0.849	0.835	0.901	0.85	0.869	0.931	0.914
2	0.805	0.787	0.805	0.830	0.885	0.910	0.884
1.75	0.770	0.750	0.799	0.770	0.864	0.893	0.86
1.5	0.741	0.729	0.740	0.773	0.846	0.897	0.838
1.25	0.725	0.714	0.716	0.727	0.735	0.751	0.820

First, after assigning G=100, we get the initial center of clustering by GA. Second, the data set was classified by FCM. Third, the value index I was evaluated. Finally, we obtained the optimum cluster number c and the classification of samples. The minimization of I is available when c is 3 and m is 1.25. Therefore, the optimum cluster number is 3. The different values of I with different c and m are shown in Table 2. Then three clusters were obtained as a result of applying GA-FCM. According to experiment performance, the three clusters corresponded to three regimes of the fluidized bed containing bubbling bed (B), slugging bed (S) and turbulent bed (T) since all data were gathered above the minimum fluidized velocity. It is not necessary to check every group of data with the corresponding original experimental conditions. It is easy to find the correspondences of some definite processes by checking the operation conditions and photos Several points of one cluster were checked, respectively, and with these points corresponding to the same regime, all points of this cluster were supposed to be the data of the same regime. The specific features of the three flow

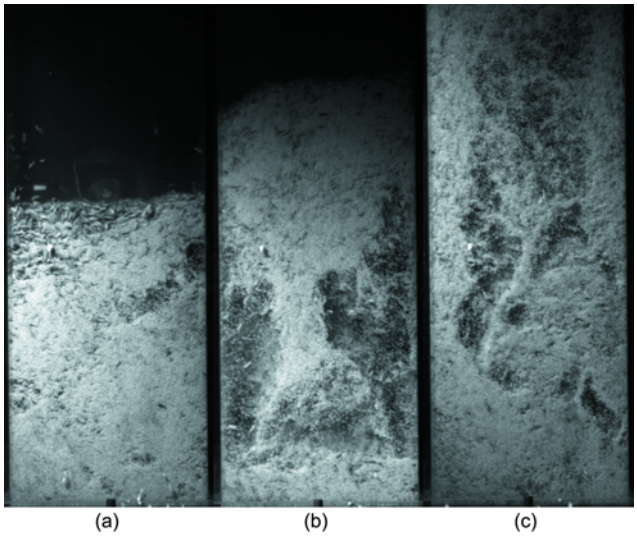

Fig. 5. The specific features of the three flow regimes in fluidized bed. (a) Bubbling bed, (b) slugging bed, (c) turbulent bed.

Table 3. The characteristic parameters of the different flow regimes

Flow regime	$P_{IMF1\text{-}3}$	$P_{IMF4\text{-}6}$
Bubbling bed	96.8149	2.8575
Slugging bed	73.0863	24.2168
Turbulent bed	39.6723	57.6974

regimes are shown in Fig. 5. The parameters of different flow regimes are shown in Table 3.

IDENTIFICATION OF THE FLOW REGIMES IN THE FLUIDIZED BED

Here we chose a multilayer neural network (4 layers: one input layer, two hidden layers, and one output layer) to train and test the identification system. With the clustered sample data from Section 3, the percentages of $IMF_{1\text{-}3}$ and $IMF_{4\text{-}6}$ were used as the input vectors. Corresponding to the input vectors, the flow regimes of each sample data were defined as the output vectors. Three different regimes (bubbling bed, slugging bed, and turbulent bed) were represented as (1, 0, 0), (0, 1, 0), and (0, 0, 1). Ninety groups of sample data were chosen as a training dataset which contained 30 groups of bubbling beds, 30 groups of slugging beds, and 30 groups of turbulent beds. The parameters of the multilayer neural network are provided in Table 4. The operation details of 90 groups of training data was given in Fig. 6.

Table 4. The parameter of the multilayer neural network

Epochs	Input layer node	Hidden layer node	Output layer node
1000	2	10	3

The other 110 groups of sample data were used as testing data and the outputs of identification were compared with the results of fuzzy c-means cluster. The operation details of 110 groups of testing data are given in Fig. 7. Table 5 was one group of the input data random chosen as an example for analysis. The output vector of example data was (0.0171, 0.0237, 0.9626), which was approximated to (0, 0, 1), so the flow regime of this group was turbulent bed. A comparison of the identifying results and the clustering results are presented in Table 6. The identification accuracies of bubbling bed regime, slugging bed regime, and turbulent bed regime were

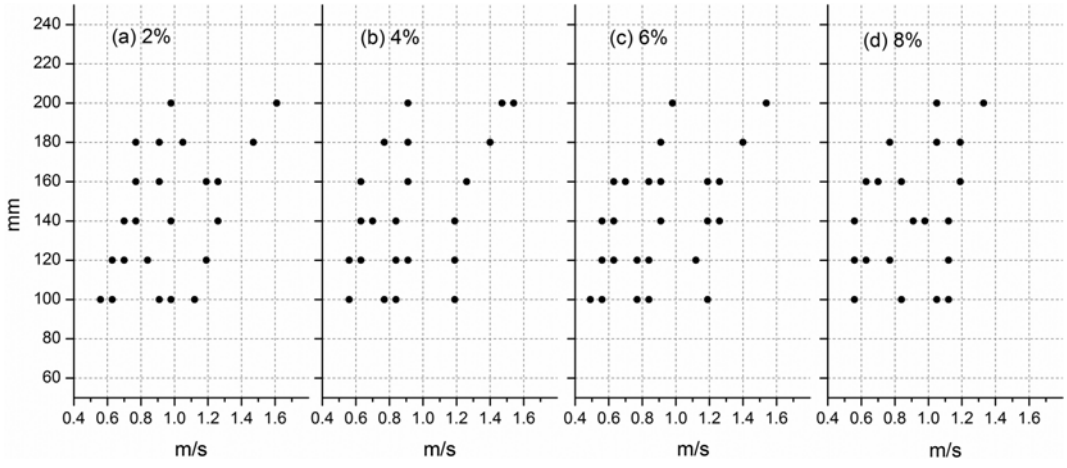

Fig. 6. The heights of bed materials and the superficial velocities of the training data.

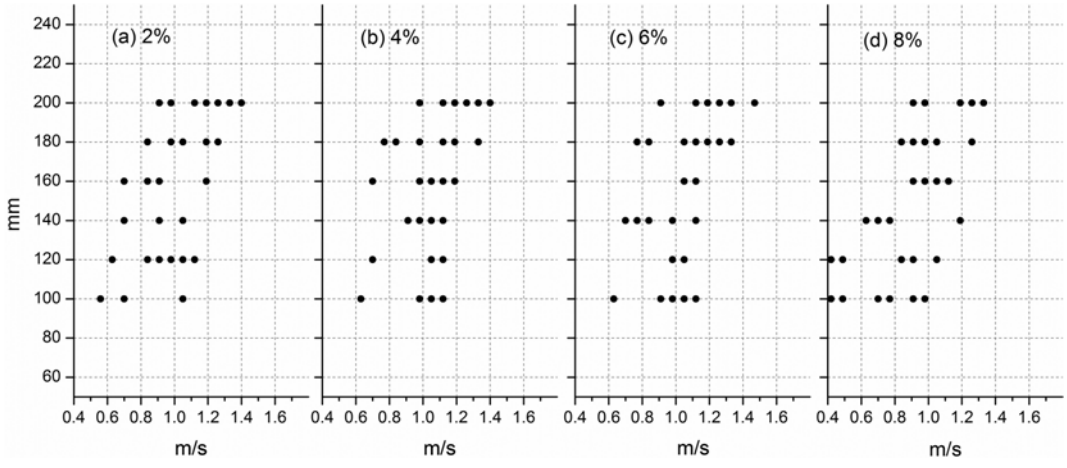

Fig. 7. The heights of bed materials and the superficial velocities of the tested data.

Table 5. Features of one analyzed sample

	$P_{IMF1\text{-}3}$	$P_{IMF4\text{-}6}$
T	27.0313	68.7313

Table 6. Comparison of the identifying results and the clustering results

	Clustering result		
	36 Groups bubbling bed	28 Groups slugging bed	46 Groups turbulent bed
Identifying result			
Bubbling bed	33 Groups	1 Groups	1 Groups
Slugging bed	2 Groups	28 Groups	3 Groups
Turbulent bed	1 Groups	1 Groups	46 Groups

91.67%, 92.86%, and 91.30%, respectively. Analyzing the data of bad identifications, we found that most errors of identification result happened when the data was sampled in the transformation of two regimes. It is acceptable because the transformations between two regimes are indefinite.

Experiments of quartz were conducted and 76 groups of data were sampled. It was very interesting that only two clusters were clustered with GA-FCM applied. According to the experiment conditions, two clusters were corresponding to two regimes, bubbling bed and turbulent bed. Trained by 40 groups, the same identification system was built to identify the regimes of quartz only system. Only two groups of data of 36 test groups failed to be identified by the trained system.

Compared with other identification methods, the intelligent identification system is more objective and automatic. In this present work, no discussion or empirical analysis was needed after the process of pressure fluctuation signals. Instead, fuzzy c-means cluster algorithm, which is the crucial step of intelligent identification system, was applied to cluster the data into several clusters automatically. The accuracy of clustering result was ensured by two improvements as mentioned in Section 3. However, this system is not perfect because the clustering part should be reloaded and the identification system should be retained when the objects changed. It is necessary to reloaded new data, but it makes the system complex. An integrated system is being built to make it easy to load data and obtain the identification results fast and easily.

CONCLUSION

A new method of identifying the flow regimes of two-component flow biomass and quartz in a fluidized bed was introduced. Fuzzy c-means clustering algorithm was applied to cluster the data samples. Genetic algorithm was applied to optimize the initial cluster center. The optimal number was introduced to represent the number of flow regimes. Three clusters were found as bubbling bed, slugging bed, and turbulent bed, respectively. A multilayer neural network was used to identify the flow regimes of two-component particles in the fluidized bed based on the results of intelligent fuzzy c-means clustering. The identification accuracies of three regimes are above 90%.

ACKNOWLEDGEMENTS

This research is supported by the National Natural Science Fund Program of China (51276040 and U1361115) and National Basic Research Program of China (2013CB228106).

REFERENCES

1. F. Duan and S. Cong, *Chem. Eng. Commun.*, **200**, 4 (2013).
2. J.-H. Choi, H.-J. Ryu and C.-K. Yi, *Korean J. Chem. Eng.*, **28**, 10 (2011).
3. F. Fotovat, J. Chaouki and J. Bergthorson, *Chem. Eng. Sci.*, 129 (2013).
4. F. X. Llauró and M. F. Llop, *Int. J. Multiphase Flow*, **32**, 12 (2006).
5. Y. M. Chen, C. J. Lim, J. R. Grace, J. Y. Zhang, Y. C. Zhao and C. G. Zheng, *Chem. Eng. Sci.*, 156 (2015).
6. R. Andreux, T. Gauthier, J. Chaouki and O. Simonin, *AIChE J.*, **51**, 4 (2005).
7. D. Bai, E. Shibuya, N. Nakagawa and K. Kato, *Powder Technol.*, **87**, 2 (1996).
8. O.-a. Jaiboon, B. Chalermsinsuwan, L. Mekasut and P. Piumsomboon, *Powder Technol.*, **233**, 215 (2013).
9. C.-h. Wang, Z.-p. Zhong, R. Li and J.-q. E, *Powder Technol.*, **205**, 1 (2011).
10. R. Ghaemi, N. bin Sulaiman, H. Ibrahim and N. Mustapha, *Artif. Intell. Rev.*, **35**, 4 (2011).
11. B. Chalermsinsuwan, T. Thummakul, D. Gidaspow and P. Piumsomboon, *Korean J. Chem. Eng.*, **31**, 2 (2014).
12. J.-H. Lim, J.-H. Shin, K. Bae, J.-H. Kim, D.-H. Lee, J.-H. Han and D. H. Lee, *Korean J. Chem. Eng.*, **32**, 9 (2015).
13. J. van der Schaaf, F. Johnsson, J. C. Schouten and C. M. van den Bleek, *Chem. Eng. Sci.*, **54**, 22 (1999).
14. C. A. S. Felipe and S. C. S. Rocha, *Powder Technol.*, **174**, 3 (2007).
15. B. Bai, S. Gheorghiu, J. R. van Ommen, J. Nijenhuis and M. O. Coppens, *Powder Technol.*, **160**, 2 (2005).
16. J. van der Schaaf, J. C. Schouten, F. Johnsson and C. M. van den Bleek, *Int. J. Multiphase Flow*, **28**, 5 (2002).
17. M. C. Shou and L. P. Leu, *Chem. Eng. Res. Des.*, **83**, A5 (2005).
18. W. Zhong and M. Zhang, *Powder Technol.*, **152**, 1 (2005).
19. B. Sun, H. Zhang, L. Cheng and Y. Zhao, *Chinese J. Chem. Eng.*, **14**, 1 (2006).
20. R. Zarghami, N. Mostoufi and R. Sotudeh-Gharebagh, *Ind. Eng. Chem. Res.*, **47**, 23 (2008).
21. X. S. Lu and H. Z. Li, *Chem. Eng. J.*, **75**, 2 (1999).
22. N. Ellis, L. A. Briens, J. R. Grace, H. T. Bi and C. J. Lim, *Chem. Eng. J.*, **96**, 1 (2003).
23. T.-Y. Yang and L.-P. Leu, *Chem. Eng. Sci.*, **63**, 7 (2008).
24. F. T. Kuhn, J. C. Schouten, R. F. Mudde, C. M. vandenBleek and B. Scarlett, *Meas. Sci. Technol.*, **7**, 3 (1996).
25. J. van der Schaaf, J. R. van Ommen, F. Takens, J. C. Schouten and C. M. van den Bleek, *Chem. Eng. Sci.*, **59**, 8 (2004).
26. J. V. Briongos, J. M. Aragon and M. C. Palancar, *Powder Technol.*, **162**, 2 (2006).
27. J. V. Briongos, J. A. Aragon and M. C. Palancar, *Chem. Eng. Sci.*,

62, 11 (2007).
28. M. Karimi, N. Mostoufi, R. Zarghami and R. Sotudeh-Gharebagh, *Chem. Eng. Sci.*, **66**, 20 (2011).
29. H. S. Ji, H. Ohara, K. Kuramoto, A. Tsutsumi, K. Yoshida and T. Hirama, *Chem. Eng. Sci.*, **55**, 2 (2000).
30. T. J. Lin, R. C. Juang, Y. C. Chen and C. C. Chen, *Chem. Eng. Sci.*, **56**, 3 (2001).
31. M. F. Llop, N. Jand, K. Gallucci and F. X. Llauró, *Chem. Eng. Sci.*, **71**, 252 (2012).
32. F. Johnsson, R. C. Zijerveld, J. C. Schouten, C. M. van den Bleek and B. Leckner, *Int. J. Multiphase Flow*, **26**, 4 (2000).
33. D. Falkowski and R. C. Brown, *Ind. Eng. Chem. Res.*, **43**, 18 (2004).
34. H. T. Bi, *Chem. Eng. Sci.*, **62**, 13 (2007).
35. S. Sasic, B. Leckner and F. Johnsson, *Progress in Energy and Combustion Sci.*, **33**, 5 (2007).
36. J. R. van Ommen, S. Sasic, J. van der Schaaf, S. Gheorghiu, F. Johnsson and M.-O. Coppens, *Int. J. Multiphase Flow*, **37**, 5 (2011).
37. N. E. Huang, Z. Shen, S. R. Long, M. L. C. Wu, H. H. Shih, Q. N. Zheng, N. C. Yen, C. C. Tung and H. H. Liu, *Proc. R. Soc. A-Math. Phys. Eng. Sci.*, **454**, 1971 (1998).
38. Z. Yang, Z. Yu, C. Xie and Y. Huang, *Measurement*, **47**, 14 (2014).
39. X. Y. Wang, Z. P. Zhong, H. Wang and Z. Y. Wang, *Korean J. Chem. Eng.*, **32**, 1 (2015).
40. C. S. Miin, S. A. Sulaiman, V. R. Raghavan, M. R. Heikal and M. Y. Naz, *Korean J. Chem. Eng.*, **32**, 11 (2015).
41. J. C. D. J. C. Bezdek, *IEEE Transactions on Computers*, 835 (1975).
42. J. C. Bezdek, R. Ehrlich and W. Full, *Computers Geosciences*, **10**, 2 (1984).